Journal of Electrical Engineering and Automation (ISSN: 2582-3051)
www.irojournals.com/iroeea/

PSO based Solar PV system for SVPWM Controlled Induction Motor for Agricultural Applications

Vivekanandhan M[1], Chitra S[2]

Department of Electrical and Electronics Engineering, Government College of Technology, Coimbatore, India

Email: [1]vivekmunirathinam2017@gmail.com,[2]eeechitra@gct.ac.in

Abstract

Nowadays, renewable energy sources play a major role in agricultural applications. The recommended Particle Swarm Optimization (PSO) algorithm with DC-DC converter supports in refining the output voltage. This is beneficial however since the partial shading condition of PSO technique has high output power with fewer searching steps of MPPT. The objective of this work is to propose a PSO based boost converter using Space Vector Pulse Width Modulation (SVPWM) method. PSO has been anticipated to track the Global Maximum Point (GMP) under the partial shading condition. The welfares of the SVPWM technique are fixed switching frequency and lower harmonic content. The centrifugal pump used in agricultural system is obsessed by SVPWM controlled three-phase induction motor. The extent of the motor as well as the photovoltaic array evaluations are certain as the water could be pumped out even at temperature fluctuations and irradiation levels. The efficacy of the proposed design is observed under the MATLAB/SIMULINK.

Keywords: Induction motor, Space Vector Pulse with Modulation, Solar PV array, MPPT, PSO, Speed control.

1. Introduction

Renewable Energy Sources have enormous potential, since they could theoretically supply much more energy than the world needs. Based on the use of commonly accessible indigenous resources, renewable energy sources such as biomass, wind, sun, hydropower, and geothermal can deliver sustainable energy services. The price of solar and wind power

DOI: https://doi.org/10.36548/jeea.2023.1.007
Received: 01.03.2023, received in revised form: 01.04.2023, accepted: 16.04.2023, published: 26.04.2023

systems has significantly decreased over the past 30 years and has continued to fall, while the price of oil and gas has continued to fluctuate, making a switch to renewable energy systems look more and more likely. In actuality, the costs associated with using renewable energy sources and fossil fuels are moving in the opposite directions [1].

In contrast to conventional energy sources, which are mostly found in a few nations, renewable energy resources are dispersed over a much greater geographic region. Clean, limitless, and more cost-effective energy comes from renewable sources. Its variety, abundance, and capacity can be used wherever on Earth set them apart from fossil fuels, but their most significant distinction is that they don't release greenhouse gases or other pollutants [3].

There are several good reasons to increase its market share in the energy sector. This power source is becoming more and more well- liked because it is flexible and has many advantages for both humans and the environment. Direct conversion of sunlight into electricity is achieved by solar cells. Solar Cells are constructed from semiconducting substances akin to those used in computer chips.

The objectives of this research are to develop a boost converter and V/f control orientation motor combo water pumping system driven by solar energy. With a PSO MPPT controller, it is possible to effectively and precisely track the highest point in a solar PV array in conditions of partial shading to put into practice the V/f control approach and raise the PV system's profitability.

2. Photovoltaic Cell

Figure 2.1 shows that the solar cells are composed by semiconductor materials like silicon which became electrically conductive when supplied by heat or light. In the semiconductor's illuminated region, the formation of pairs of hole electrons occurs. As a result, the conduction band electronics are now liberated to move in any direction thanks to the PV cells' electric field. By connecting metal plates on the top and bottom of the PV cell, the current created by these moving electrons, which form current, can be used externally. Due to the electric fields already present, this current and voltage generate the necessary power. The solar cell efficiency depends on the irradiation of the solar.

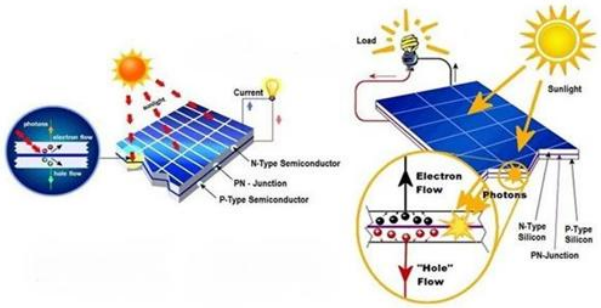

Figure 2.1. Solar PV panel

Table 2.1 describes the different parameters of solar panels and ratings, and the Boost converter parameters are described in Table 2.2

Table 2.1 Parameters of solar panels and ratings

PARAMETERS	**RATINGS**
Solar PV1 array	60.48V
Solar PV2 array	58.6
Maximum power at PV1	1.974 KW
Maximum power at PV2	1.875 KW
maximum point (voltage)	60V
maximum point (current)	8A
Output voltage	392V

Table 2.2 Boost converter parameters

PARAMETERS	**RATINGS**
Boost converter inductance	0.06975
Boost converter capacitance	0.003875
Switching Frequency	5KHZ

CHARACTERISTICS OF PV CELL

Figure 2.2 shows that Voc, Ish, and maximum power point are the three main components of the PV characteristics. At the maximum power point, a PV cell can produce its greatest amount of power. While it can create a basic model using these parameters, more

data is needed to create a model that is correct. I-V and P-V characteristics are shown in figure 2.2.

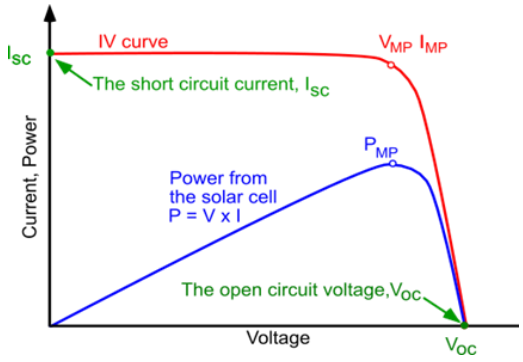

Figure 2.2. Characteristics of a PV

3. BOOST CONVERTER

Here the panel output is given to this converter. A circuit diagram of boost converter (DC-DC) is shown in Figure 3.1. Solitary a switch, which typically uses a transistor family expedient, is depicted. Moreover, a diode is linked in series to the load. The burden is of the same kind as the one that was previously mentioned. The load's inductance is minimal. An inductance, L, is presumptively connected in series with the input supply.

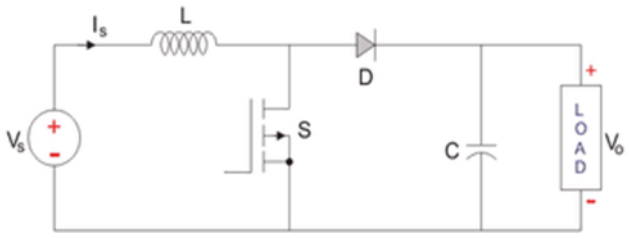

Figure 3.1. Circuit diagram of Boost converter

The switch S is instantly turned on at the beginning. If there is no battery (back emf) connected in series with the load and the load inductance is modest, the output voltage is zero (Vo=0). The inductance L receives electricity from the source and conducts it. In this interval, the value of current rises linearly with time and (di/dt) is positive. The induced emf is assumed to have a positive polarization as the current through L rises, with positive being associated with L's left side. The circuit's equation is,

$$V_l = L \, dis / dt \quad or \; dis/dt = Vs/L \qquad (1)$$

The switch, S, is turned off during the time, T, with OFF standing for TOFF. T-TON- is the duration (T- TON+TOFF) as L experiences a reduction in current. The generated emf reverses, such that the left side of L becomes negative, and its orientation is in the same direction. As a result, the supply voltage is added to the induced emf with the same polarity, maintaining the current. (Is=Io). Voltage is assumed to be nearly constant at Vs=Vo with (dis/dt) being negative as Vs<Vo.

$$I_2 - I_1 = I_{max} - I_{min}[(V_o - V_1)/L]T_{OFF} \quad (2)$$

Equating the above equations,

$$(V_s/L)T_{ON} = [(V_o - V_s)/L]T_{OFF} \quad (3)$$

The average output voltage, $V_o = V_s(T/T_{ON}) = V_s(T/T - T_{ON})$

$$V_o = V_S(1/1-(T_{ON}/T)) = V_S(1/(1-k)) \quad (4)$$

The time period is,

$$T = T_{ON} + T_{OFF} \quad (5)$$

Duty cycle is given by,

$$k = (T_{ON}/T) = (T_{ON}/(T_{ON}+T_{OFF})) \quad (6)$$

The ON time is TON-kT. The range is shortened, as mentioned in the prior instance. As the smallest value is greater than the minimum and the highest value is lower than the extreme (1.0), the source current is presumed to be continuous for the reasons stated there, which are also applicable here. Other methods can be used to obtain the expression for the output voltage.

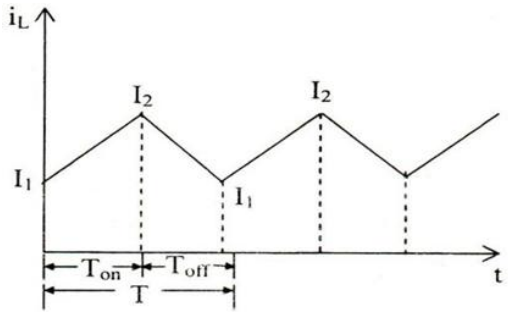

Figure 3.2. Waveform of source current

In contrast to the preceding buck converter situation, the output voltage in this instance is higher than the input voltage (DC-DC). When a nature- commutated device is employed as a switch, this is referred to as a boost converter (DC-DC). Step-up chopper is the name used when thyristor is utilized in its place. It is simple to calculate the output voltage's variation. The output voltage of the solar panel is increased by using the boost converter to vary the duty cycle of the boost converter. After boosting the voltage is fed to the three phase induction motor to run the agricultural pump by using the SVPWM controller.

4. Algorithm and Control Technique

4.1 Maximum Power Point Tracking

The solar panel must be tracked to maximise efficiency. MPPT is a technique that accounts for the solar panel's fluctuating voltage and current characteristics while maximising solar energy output. The MPPT is the point where solar panel output is at its highest and solar cell efficiency is increased. It has an electronic system that controls the PV modules in a way that lets them generate all the power. Many methods are employed to track the maximum power. The technique is effective to track maximum power depending on implementation cost, time, and complexity [4].

4.2 Particle Swarm Optimizarion

1.The goal of particle swarm optimisation is to increase the solar system's MPPT capabilities under the partial shading condition. The PSO algorithm keeps track of numerous prospective solutions simultaneously [5]. Each solution is assessed by an objective function during each iteration of the algorithm to determine its fitness. The PSO algorithm's primary goal benefits when utilizing a PV system.

2. There is a significant reduction in tuning effort because only one parameter, the inertia weight, w, needs to be adjusted.

3. When compared to the traditional PSO, the approach greatly simplifies the optimization structure. It reduces the amount of computing needed and is simple for a cheap microprocessor to implement.

4. In a variety of environmental situations, such as those seen in tropical nations, V max can be highly valuable. The frequent presence of clouds in tropical regions causes frequent changes in P-V curves. For reliable tracking, the values of duty cycles can be gently increased or lowered in two subsequent M_iPPT cycles by adjusting the value of V max. Although the searching speed is typically slower, GP tracking is indeed available.

The following equations that specify a particle's position and velocity together represent the PSO method mathematically.

$$U_i^{k+1}=wu_i^k+C_1r_1(P_{besti}-X_i^k)+C_2r_2(G_{best}-X_i^k) \quad (7)$$

$$Xik=x\ k+uik \quad (8)$$

Where,

u_i^k is the velocity of individual i at iteration k, w is an inertia weight parameter k, c1 and c2 are acceleration coefficients, r1 and r2 are random numbers between 0 and 1, x is where individual I is at iteration k,

pbest is where individual I is at its best at iteration k, and gbest is where the group is at its best up to iteration k.

Either an equation or a preset value can be used to determine the value of w. Vref is first set to a certain value in the first iteration. Then it is modified in accordance with (7) and (8). By multiplying the observed voltage (Vpv) and current, the power Pp is determined (pv). The system then assesses the following equation to see superior-individual fitness value produced by the voltage-reference value.

$$P_{pv,i}>P_{pv,}\ i\text{-}1 \quad (9)$$

The global fitness value (gbest) is then examined in relation to the power of the other particles to see whether it needs to be updated. Each particle needs to have enough time to do all the aforementioned tasks. To guarantee that all the particles converge to the GMP, the convergence criterion as given in (2) is tested.

$$Ppv.gbest-Ppv.il\ l< Ɛ1;\ i=1....n, \quad (10)$$

where Ɛ, is the tolerance value.

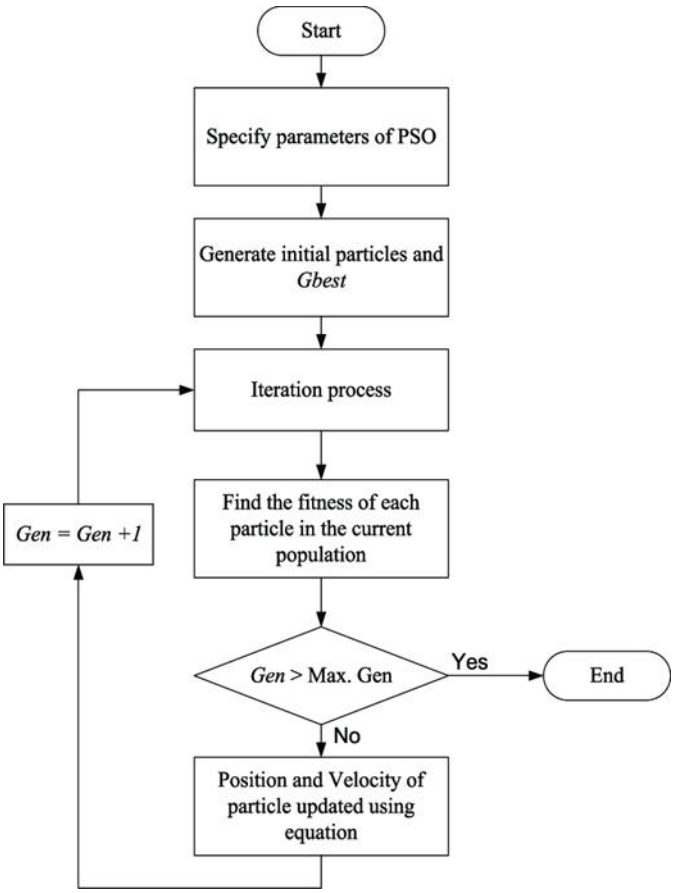

Figure 4.1. Flowchart for PSO algorithm

For induction motor, the SVPWM technique is best because of fixed switching frequency, low harmonic content and higher DC bus voltage utilization. There are eight possible switching configurations when using space vector modulation for motor control on a three-phase inverter with six switches, as shown by the analogous circuit below.

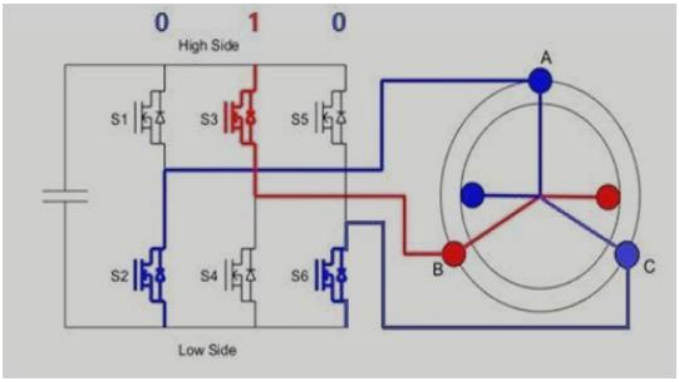

Figure 4.2. An equivalent circuit for the inverter's switching sequence

To the motor terminals is applied a particular voltage depending on the switching configuration. The voltages are fundamental space vectors, and a space vector hexagon represents their magnitude. It is possible to approximate a voltage vector of any magnitude, at any location within the space vector hexagon, by combining the switching states that correspond to the fundamental space vectors and the null vectors.

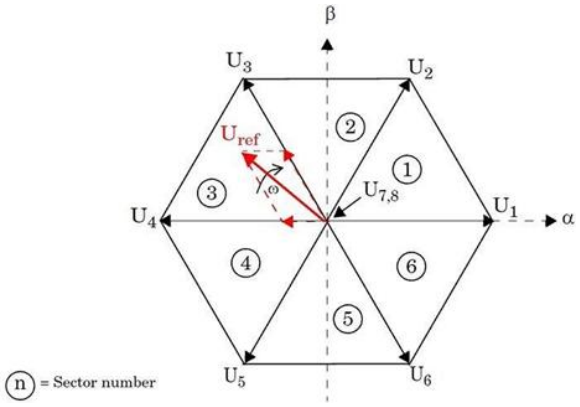

Figure 4.3. Space vector hexagon with basic vectors U1-U8

By adjusting the switching order and the ON time duration of pulses, any voltage vector with different amplitude and direction is conceivable for every PWM period. The space vector modulation technique generates switching sequences that match the reference voltage vector for each PWM period, resulting in a space vector that rotates continuously. The double hump in the modulation wave that is generated, maximizes the use of the DC bus voltage that is available. When compared to the Sinusoidal Pulse Width Modulation (SPWM) approach, this offers a higher rated voltage output.

5. INDUCTION MOTOR- V/F CONTROL

By changing the supply frequency, synchronized speed can be managed.

Where, is the air-gap flux and f is the supply frequency. The voltage induced in the stator is equal to 1f. The terminal voltage V1f is obtained by ignoring the stator voltage loss. Hence, lowering the frequency without altering the supply voltage will result in an unfavourable increase in air-gap flux. Table 5.1 below tabulates the ratings and characteristics of induction motor.

Table 5.1 Parameters of induction motor

PARAMETERS	**RATINGS**
Input voltage	400V
Inverter output AC voltage	400V
Induction motor rating	5.4HP (or) 4KW
Voltage	400V
Frequency	50HZ
Speed	1430rpm
Input torque (Step)	0-3Nm
Reference speed	130-160rps

In order to maintain a consistent V/f ratio, frequency is changed anytime to control speed, and the terminal voltage is likewise changed. Hence, the maximum torque of the motor is constant for changing speed by maintaining a constant V/f ratio

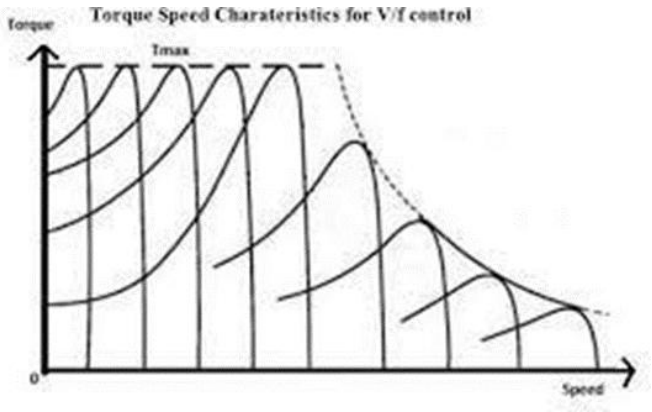

Figure 5.1. Torque speed characteristics for V/f controlled induction motor [9]

6. Simulation Results

The MATLAB-Simulink software has been used to create a water pumping system powered by renewable energy. MATLAB is currently a full-fledged technical computer environment. The Simulink (Simulation and Link) is an extension of working in MATLAB by Math. It collaborates with MATLAB to provide Graphical User Interface (GUI)-based modelling, simulation, and analysis of dynamical systems.

7. Simulation for Pso Based Solar Mppt Algorithm

The PSO based solar MPPT was implemented by using the MATLAB Simulink which is shown in figure 7.1. Voltage and current at the maximum point are shown in Figure 7.2. The output voltage of solar panel is shown in Figure 7.3 describing the output voltage of the solar panel.

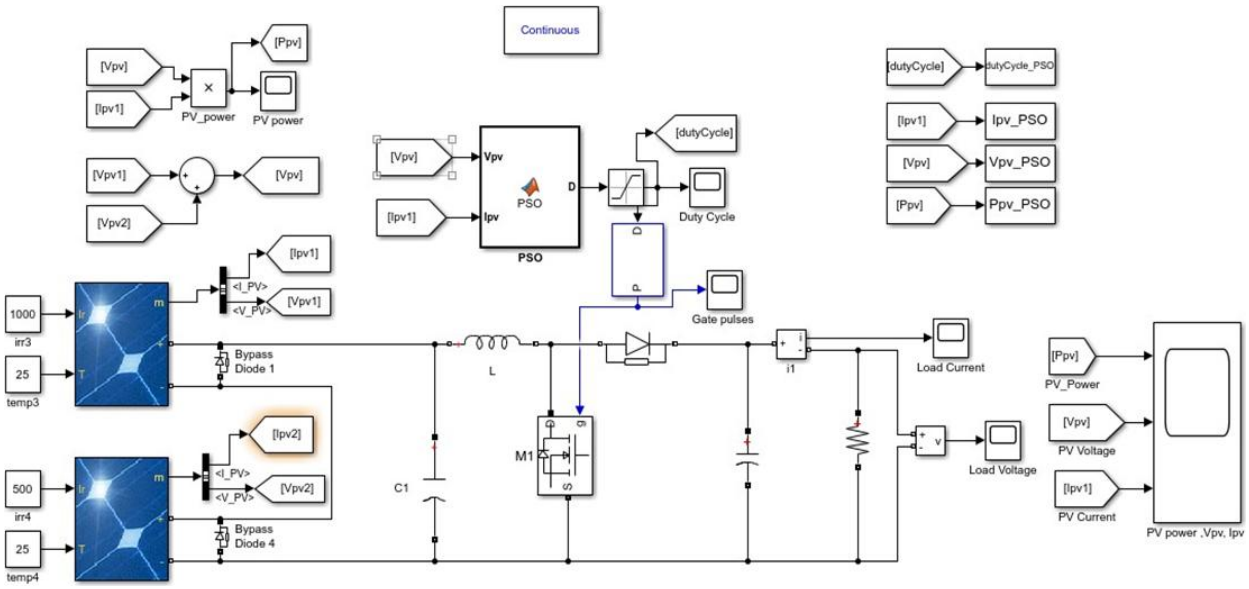

Figure 7.1. Simulation for PSO based solar MPPT algorithm,

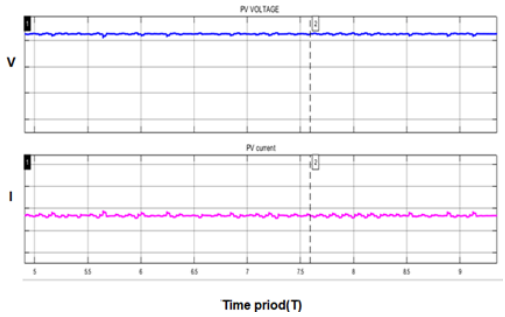

Figure 7.2. Voltage and current at maximum point

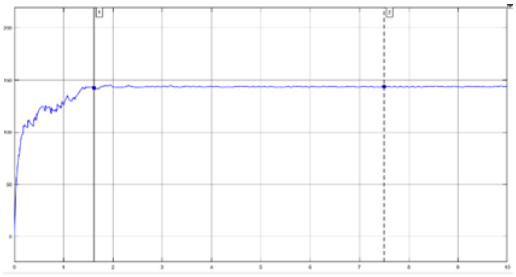

Figure 7.3. Output voltage of solar panel

8. Speed Control of Induction Motor

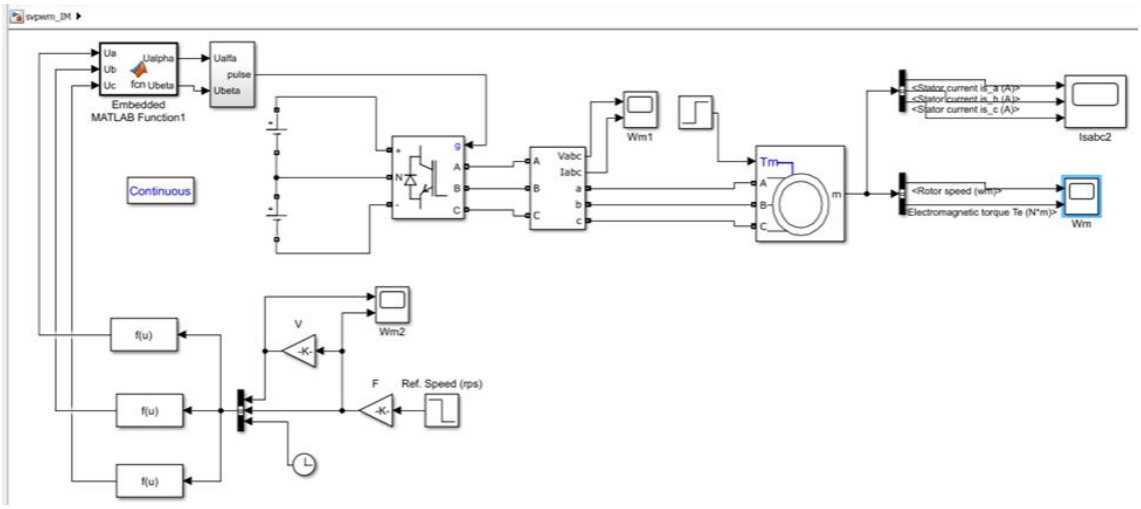

Figure 8.1. Simulation for speed control of induction motor

9. Simulation Outputs for Induction Motor

The output voltage and current of inverter are shown in Figure 9.1, which shows that the three phase voltages are Va, Vb, Vc and the three phase currents are Ia, Ib,

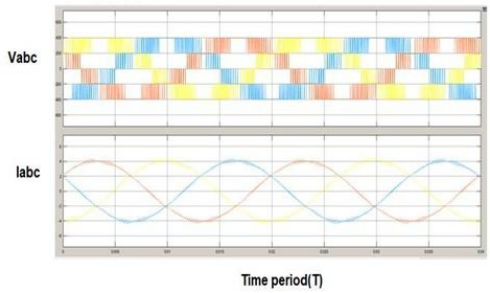

Figure 9.1. Output voltage and currents of inverter

The stator current of induction motor is shown in Figure 9.2 that describes the three phase stator current waveforms with respect to time.

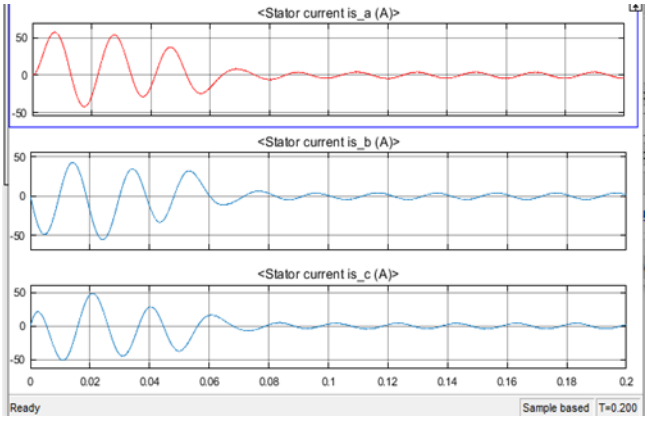

Figure 9.2. Stator currents of induction motor

The induction motor speed is shown in Figure 9.3 describing that the speed increases linearly with respect to time.

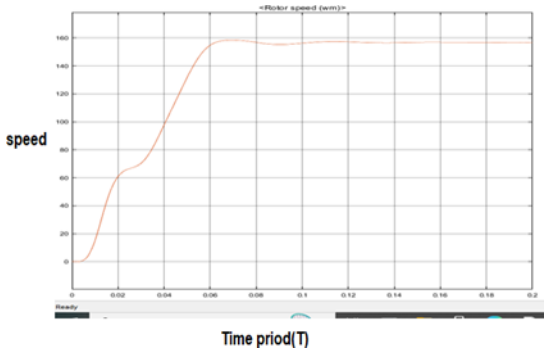

Figure 9.3. Speed of induction motor

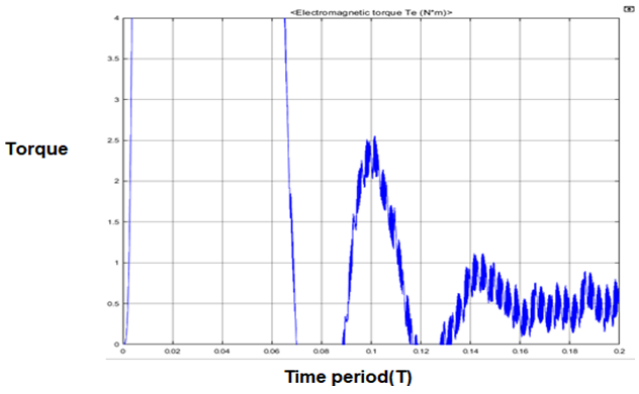

Figure 9.4. Torque characteristics of induction motor

The torque characteristics of the induction motor is shown in Figure 9.4 which describes the mechanical characteristics.

The torque characteristics shown in Figure 9.4 are listed in the below Table.

Table 9.1 Torque characteristics with time

TIME(S)	TORQUE(N-M)
0.1	2.5
0.2	0.8

10. Conclusion

The pump can be powered by a solar panel-powered induction motor. In order to convert the DC voltage from the PV array into sinusoidal AC voltage, this drive uses a VSI inverter. SVPWM pulses are used to turn specially built MOSFET switches on. The PSO MPPT controller is used to actualize the MPPT calculation in order to extract the most power possible from the PV array. The induction motor functions as efficiently as possible thanks to the V/f control process. From this research, it can be inferred that PV-powered water pumping can be used in rural areas without electricity to deliver the water needed for irrigation and general consumption.

References

[1] Y.-H. Liu, S.-C. Huang, J.-W. Huang, and W.-C. Liang, 2012 "A particle swarm optimization-based maximum power point tracking algorithm for PV systems operating under partially shaded Energy Convers., vol. 27, no. 4, pp. 1027-1035.

[2] K. Ishaque and Z. Salam, 2013. "A deterministic particle swarm optimization maximum power point tracker for photovoltaic system under partial shading condition," IEEE Trans. Ind. Electron., vol. 60, no. 8, pp. 3195- 3206.

[3] Periasamy, N. K. Jain, and I. P. Singh,2015 “A review on development of photovoltaic water pumping system”, Renewable Sustain. Energy Rev., vol. 43, pp. 918–925.

[4] Liu, Y. Chen, J., Huang, 2013 “Global maximum power point tracking algorithm for PV systems operating under partially shaded conditions using the segmentation search method”, Sol. Energy,103, pp. 350-363.

[5] K.Ishaque, Z. Salam, M. Amjad, and S. Mekhilef, Aug. 2012 An improved particle swarm optimization (PSO)-based MPPT for PV with reduced steady state oscillation" IEEE Trans. Power Electron., vol. 27, no. 8, pp. 3627-3638. Y.-

[6] H. Liu, S.-C. Huang, J.-W. Huang, and W.-C.

[7] M. T. A. Khan, G. Norris, R. Chattopadhyay,I. Husain and S. Bhattacharya, March-April 2017 “Autoinspection and Permitting With a PV Utility Interface (PUI) for Residential Plug-and-Play Solar Photovoltaic Unit,” IEEE Trans. Ind. Appl., vol. 53, no. 2, pp. 1337-1346.

[8] E. Drury, T. Jenkin, D. Jordan, and R. Margolis,Jan. 2014 "Photovoltaic investment risk and uncertainty for residential customers," IEEE J. Photovolt., vol.4, no. 1, pp. 278-284.

[9] Rajan kumar,bhim singh,2019”Solar pv powered-sensorlessBLDC motor”. DOI:10.1049/iet-rpg.2018.5717,IET Renewable power Generations, Vol. 13 Iss. 3, pp. 389-398, ISSN 1752-1416.

[10] U. Sharma, S. Kumar, and B. Singh, 2016 "Solar array fed water pumping system using induction motor drive," in Proc. 1st IEEE Intern. Conf. Power Electron., Intell. Control Energy Syst., Delhi, India, pp.1-6.

[11] U. Sharma, S. Kumar, and B. Singh, 2016 "Solar array fed water pumping system using induction motor drive," in Proc. 1st IEEE Intern. Conf. Power Electron., Intell. Control Energy Syst., Delhi, India, pp.1-6.

[12] T. Franklin, J. Cerqueira, and E. de Santana, Sep. 2014 "Fuzzy and Pl controllers in pumping water system using photovoltaic electric generation," IEEE Trans. Latin Amer., vol. 12, no. 6, pp. 1049-1054.

[13] R. Kumar and B. Singh, , May/Jun, 2016" BLDC motor-driven solar PV array-fed wa-ter pumping system employing zeta converter," IEEE Trans. Ind. Appl., vol. 52, no. 3, pp. 2315-2322.

[14] S. Jain, A. K. Thopukara, R. Karampuri, and V. T. Somasekhar, Sep. 2015 "A single- stage photovoltaic system for a dual-inverter-fed open-end winding induction motor drive for pumping applications, "IEEE Trans. Power Electron., vol. 30, no. 9, pp. 4809-4818.

[15] J. Caracas, G. Farias, L. Teixeira, and L. Ribeiro, Jan/Feb. 2014 "Implementation of a high-efficiency, high-lifetime, and low-cost converter for an autonomous photovoltaic water pumping system, "IEEE Trans. Ind. Appl., vol. 50, no. 1, pp. 631-641,.

[16] R. Antonello, M. Carraro, A. Costabeber, F. Tinazzi, and M.Zigliotto, , Jan. 2017 "Energy-efficient autonomous solar water-pumping system for permanent- magnet synchronous motors, IEEE Trans. Ind. Electron., vol. 64, no. 1, pp. 43-51.

[17] M. Calavia 1, J. M. Peri' e1, J. F. Sanz, and J. Sall' an, .2010 "Comparison of MPPT strategies for solar modules," in Proc. Int. Conf. Renew. Energies Power Quality, Granada, Spain, Mar. 22-25, pp. 1440-1445.

[18] Trishan Esram and P. L. Chapman, Jun. 2007 "Comparison of photovoltaic array maximum power point tracking techniques, "IEEE Trans. Energy Con-vers.,vol. 22, no. 2, pp. 439-449.

[19] B. Subudhi and R. Pradhan, Jan. 2013 "A comparative study on maximum power point tracking techniques for photovoltaic power systems, "IEEE Trans. Sustain. Energy, vol. 4, no. 1, pp. 89-98. Garrigos, J. Blanes, J. Carrascoa, and J. Ejea,2007"Real time estima-tion of photovoltaic modules characteristics and. its application to max-imum power point operation," Renew. Energy, vol. 32, pp. 1059-1076.